LETTERS

Cool heliosheath plasma and deceleration of the upstream solar wind at the termination shock

John D. Richardson[1,2], Justin C. Kasper[3], Chi Wang[2], John W. Belcher[1] & Alan J. Lazarus[1]

The solar wind blows outward from the Sun and forms a bubble of solar material in the interstellar medium. The termination shock occurs where the solar wind changes from being supersonic (with respect to the surrounding interstellar medium) to being subsonic. The shock was crossed by Voyager 1 at a heliocentric radius of 94 AU (1 AU is the Earth–Sun distance) in December 2004 (refs 1–3). The Voyager 2 plasma experiment observed a decrease in solar wind speed commencing on about 9 June 2007, which culminated in several crossings of the termination shock between 30 August and 1 September 2007 (refs 4–7). Since then, Voyager 2 has remained in the heliosheath, the region of shocked solar wind. Here we report observations of plasma at and near the termination shock and in the heliosheath. The heliosphere is asymmetric, pushed inward in the Voyager 2 direction relative to the Voyager 1 direction. The termination shock is a weak, quasi-perpendicular shock that heats the thermal plasma very little. An unexpected finding is that the flow is still supersonic with respect to the thermal ions downstream of the termination shock. Most of the solar wind energy is transferred to the pickup ions or other energetic particles both upstream of and at the termination shock.

The first crossing of the termination shock, by Voyager 1, defined the scale size of the heliosphere; the second crossing, by Voyager 2, reveals the scale of the heliospheric asymmetry. Both termination shock crossings were foreshadowed by observations of streaming energetic particles upstream of the termination shock, in the region named the foreshock in analogy with planetary magnetospheres. Voyager 1, at heliographic latitude 34° N, entered the termination foreshock region at helioradius 85 AU and crossed the termination shock at helioradius 94 AU. Voyager 2, at heliolatitude 26° S, entered the foreshock region at helioradius 75 AU and crossed the termination shock at helioradius 84 AU (see Figs 1, 2 and 3). The spacecraft are

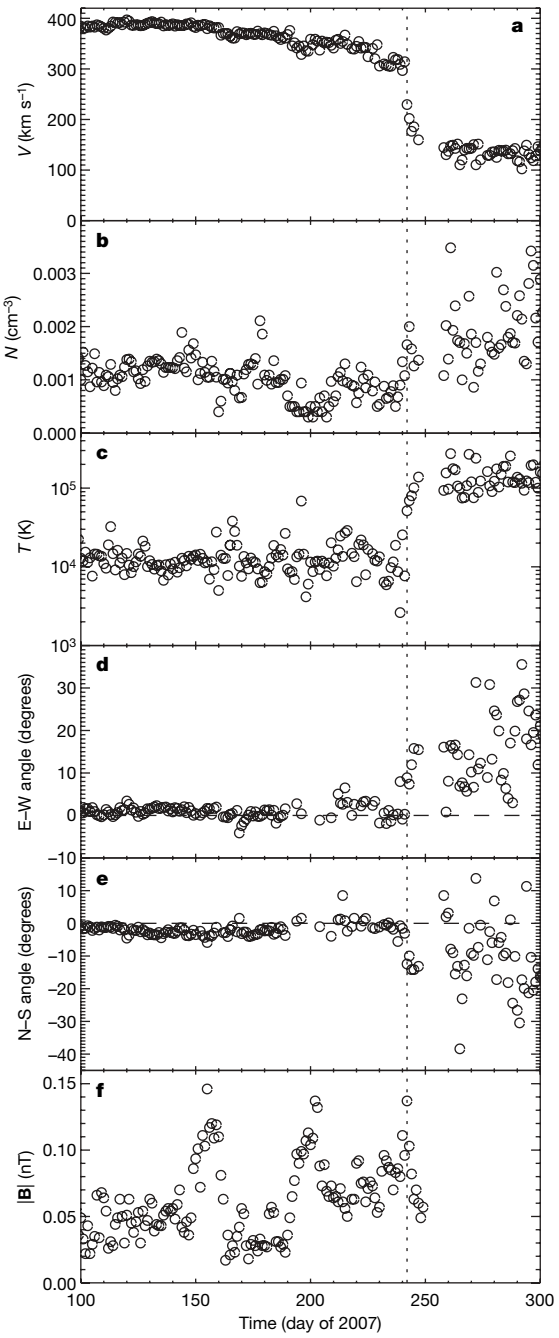

Figure 1 | An overview of data near the termination shock. Daily averages of solar wind speed *V* (**a**), density *N* (**b**), temperature *T* (**c**), east–west flow angle (**d**), north–south flow angle (**e**) and magnetic field magnitude (**f**). Flow angles are in the RTN coordinate system, where R is radially outwards, T is parallel to the plane of the solar equator and positive in the direction of the Sun's rotation, and N completes a right-handed system. The east–west angle is the angle in the R–T plane and the north–south angle is the angle out of the R–T plane. The dashed line shows the termination shock crossing, where the speed decreases by a factor of about two, the density increases by a factor of two, the proton temperature increases to near 100,000 K, and the flow is deflected in the +T and –N directions, consistent with flow away from the nose direction of the heliosphere, that is, the direction toward the local interstellar medium flow. The Voyager plasma experiment measures ions and electrons with energy per electron charge of 10–5,950 eV (ref. 8). Sets of ion and electron spectra were obtained every 192 s; these spectra are fit with convected isotropic maxwellian distributions to determine the plasma velocity, density and temperature.

[1]Kavli Institute for Astrophysics and Space Research, Massachusetts Institute of Technology, 37-655, Cambridge, Massachusetts 02139, USA. [2]State Key Laboratory of Space Weather, Center for Space Science and Applied Research, Chinese Academy of Sciences, PO Box 8701, Beijing 100080, China. [3]Harvard-Smithsonian Center for Astrophysics, 60 Garden Street, Cambridge, Massachusetts 02138, USA.

about 45° apart in heliolongitude and are separated by roughly 110 AU. The nearer foreshock boundary, in the Voyager 2 direction, was attributed to the combined effects of a thicker foreshock region in the direction of Voyager 2 and a termination shock that is closer to the sun towards Voyager 2 than it is towards Voyager 1 (refs 7, 8). Interpretations of the interstellar hydrogen and helium flow directions[9,10] and heliospheric radio emissions[11] suggest that the interstellar magnetic field is tilted at 60° from the flow direction of the interstellar medium, which would push the southern portion of the heliosphere inwards relative to the northern portion[7,12], although the magnitude of this asymmetry has been disputed[8,13].

The Voyager 2 data resolve this dispute: Voyager 2 crossed the termination shock 10 AU closer to the Sun than did Voyager 1. However, the termination shock position changes with the solar wind pressure: stronger solar wind pushes the termination shock farther from the Sun. We use the solar wind pressures observed by Voyager 2 before the termination shock crossing and a two-dimensional magnetohydrodynamics model[14] to calculate the motion of the termination shock from the time of the Voyager 1 crossing to that of the Voyager 2 crossing. The termination shock should move in by 2–3 AU owing to solar wind pressure changes; thus, the asymmetry of the termination shock is 7–8 AU, with the shock closer to the Sun in the Voyager 2 direction than it is in the Voyager 1 direction (which could be an east–west or north–south asymmetry, or both).

The first effects of the termination shock on the solar wind speed occurred 0.7 AU upstream of the shock and were very large in comparison with foreshock effects upstream of planetary magnetospheres (see Figs 1 and 4). The solar wind speed decreased from 400 to 300 km s^{-1} in three steps. These steps seemed to be associated with magnetic field enhancements that could be either transient structures or standing waves. Roughly 40% of the bulk energy of the solar wind flow is dissipated before the shock in these speed decreases.

The termination shock was a supercritical quasi-perpendicular shock (see Table 1). The shock curvature is smaller than for a circular shock; this curvature may be due to small-scale oscillations, as the overall shock is expected to be blunt[15]. The shock widths were 300,000 km for TS-2 and 100,000 km for TS-3. These widths are a few times the ion inertial length and are much larger than the electron inertial length and the thermal ion gyroradius.

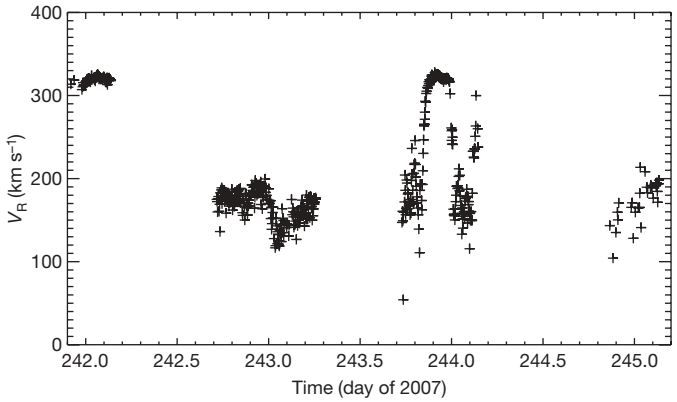

Figure 2 | High-resolution (192 s) solar wind speed (V_R) near the termination shock crossings. At the end of the tracking pass at the beginning of day 242, Voyager 2 was in the solar wind. When tracking resumed at day 242.7, the spacecraft had entered the heliosheath; the first TS crossing (TS-1) occurred in this data gap. Voyager 2 remained in the heliosheath until day 243.85, when the termination shock moved outwards past the spacecraft (the second termination shock crossing, TS-2). Voyager 2 was in the solar wind for about three hours; then the termination shock moved back inward across the spacecraft (TS-3). Another termination shock crossing or partial crossing (TS-4) occurred when the shock again moved outwards at day 244.1. Voyager 2 was in the heliosheath when tracking resumed at the end of day 244 (TS-5 occurred in this gap) and has remained in the heliosheath since that time.

The weakness of the termination shock, with shock compression ratios of 2.4 at TS-2 and 1.6 at TS-3, and the lack of plasma heating at the shock distinguish it from planetary bow shocks, where most of the flow energy is transferred to the thermal plasma (see Fig. 5). The electron temperature at the termination shock also increased by an order of magnitude less (to 3×10^4–4×10^4 K) than at planetary bow shocks. If all the flow energy were transferred to the thermal ions as happens at planetary bow shocks, the heliosheath temperature

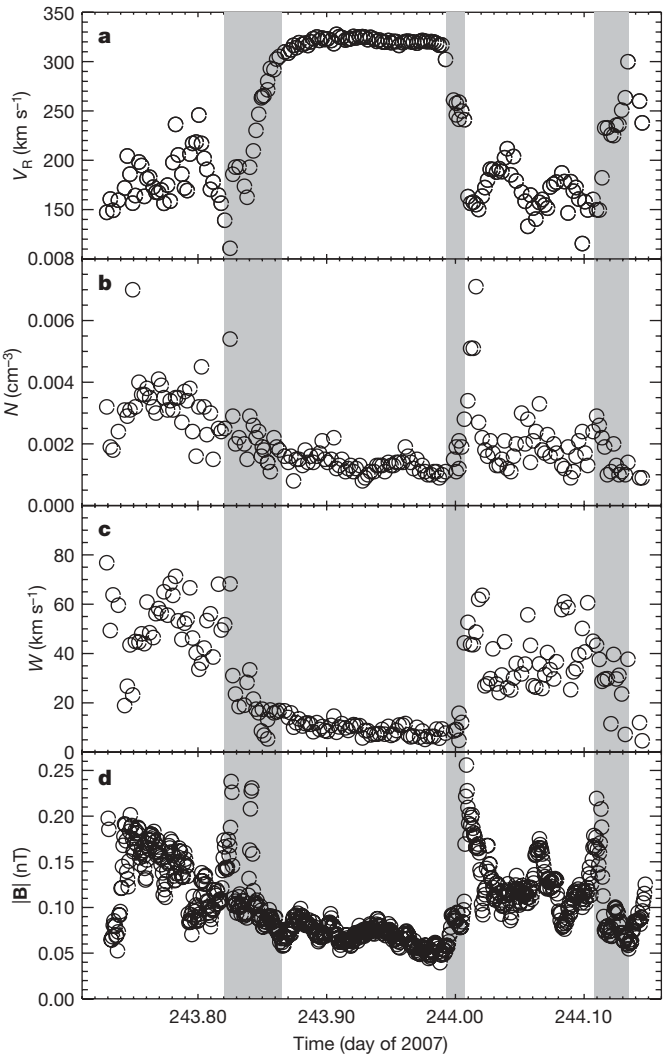

Figure 3 | High-resolution data near the termination shock crossings (shaded regions). Solar wind speed (**a**), density (**b**), thermal speed W (**c**) and magnetic field magnitude (**d**). TS-2, which began at day 243.85, lasted ~1 h. The solar wind speed increased from 150 km s^{-1} to 325 km s^{-1}. The density decreased over a more extended region, from day 283.75 to 283.865, and did not show a sharp jump. The temperature decrease was sharp, but occurred before the speed change and coincided with a peak in the magnetic field strength. The spectra remained roughly maxwellian throughout this period, so plasma changes at the shock occurred on timescales longer than an ion gyroradius. TS-3, at day 244.0, had the structure of a classic supercritical quasi-perpendicular shock[4]. The speed decreased in two steps, first to 250 km s^{-1} in the region called the shock foot, where $|\mathbf{B}|$ also increased, and then to 150 km s^{-1} at the ramp, the transition to the heliosheath. The density also increased in the shock foot and then again in the heliosheath; the temperature increase occurred at the ramp. About 14 min after the ramp, the heliosheath density increased by a factor of >3 for a few spectra; this feature is not understood. Other very small-scale features are observed in the heliosheath density near the termination shock (for example the single-point peak at day 243.74); these features are real but their source is not known. The crossing at day 244.12 also seems to show a foot–ramp structure; this event may not be a full crossing of the shock but is at least a close encounter.

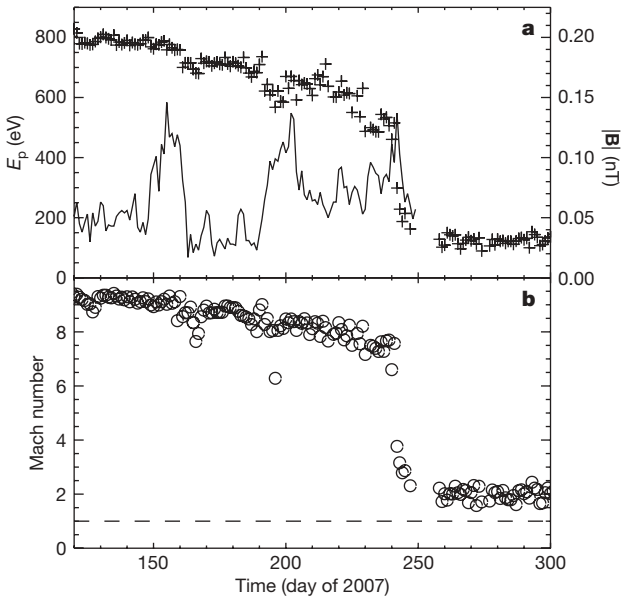

Figure 4 | Most of the solar wind flow energy does not go into the solar wind plasma. **a**, Daily-averaged energy per proton E_p (flow energy plus thermal energy; crosses) near the termination shock, with the magnitude of **B** (continuous trace) superposed. Stepped decreases in energy occurred at days 160, 190 and 230; the first two coincided with increases in the magnetic field strength. **b**, The fast-mode Mach number near the termination shock. The Mach number, the speed divided by the fast-mode wave speed of the thermal plasma, is about nine before the shock and two after the shock. The dashed line shows a Mach number of one. The Mach number was expected to be less than one after the shock.

would be 10^6 K, whereas the observed temperature is 10^5 K. The small temperature increase results in heliosheath flow that is not subsonic with respect to the thermal plasma (see Fig. 4). However, the effect of a shock is to make the flow subsonic (Mach number <1). We explain this discrepancy as follows. The energy per proton decreases by 80% at the termination shock, so the solar wind flow energy is not going into heating the thermal plasma as in planetary bow shocks. This energy is probably transferred to the pickup ions, which are hot protons created when neutral interstellar particles are ionized in the heliosphere. The Voyager 2 plasma data and extrapolations of Voyager 1 energetic particle data to pickup ion energies in the heliosheath are consistent with roughly 80% of the solar wind flow energy being transferred to the pickup ions[16,17]. The wave speeds in the heliosheath would then be determined by the properties of the hot pickup ions, not the thermal plasma, and would be faster than the flow speed, resulting in the heliosheath being subsonic. Particle code models including pickup ions seem consistent with this explanation[18,19].

Table 1 | Termination shock parameters

Parameter	Termination shock motion	
	TS-2: outwards	TS-3: inwards
East–west shock normal angle	$188.0^\circ \pm 4.0^\circ$	$5.8^\circ \pm 10.3^\circ$
Shock speed	94.0 ± 3.4 km s^{-1}	67.9 ± 17.3 km s^{-1}
North–south shock normal angle	$2.0^\circ \pm 6.2^\circ$	$-4.6^\circ \pm 19.2^\circ$
Angle between shock normal and magnetic field	$82.8^\circ \pm 3.9^\circ$	$74.3^\circ \pm 11.2^\circ$
Compression ratio	2.38 ± 0.14	1.58 ± 0.71
Solar wind fast-mode Mach number	4.9 ± 0.1	8.8 ± 1.2
Heliosheath fast-mode Mach number	1.1 ± 0.1	2.8 ± 0.4

The termination shock parameters derived from the Voyager 2 data. We assume that the termination shock is locally planar and described by the fluid magnetohydrodynamics equations. The change in the plasma parameters across the shock must satisfy the Rankine–Hugoniot jump conditions. The most probable orientation of the termination shock is the direction that minimizes the differences of the Rankine–Hugoniot conditions across the shock[20–23]. Once the orientation is determined, the shock speed, the angle between the shock and the magnetic field, the wave speeds, and the Mach numbers are calculated.

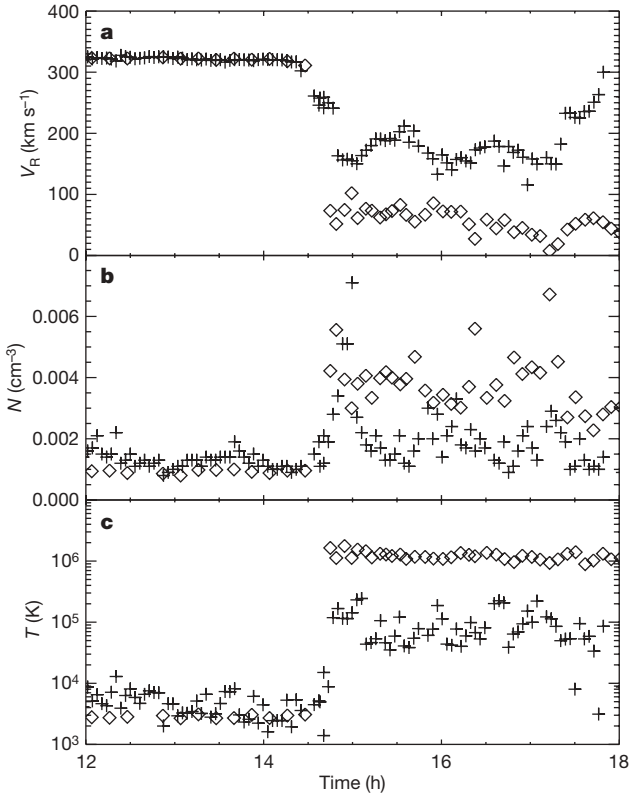

Figure 5 | The termination shock is very different from other shocks observed in the heliosphere. Voyager 2 data measured at TS-2 (crosses) at helioradius 84 AU, in comparison with Voyager 2 data measured at Neptune's inbound bow shock crossing (diamonds) at helioradius 30 AU in August 1989. The solar wind parameters upstream of Neptune are normalized to those upstream of the termination shock; the timescales are identical. The solar wind speed (**a**; Neptune data divided by 1.3) at the bow shock fell by a factor of four but at the termination shock the speed decreased by a factor of only two. The density (**b**; Neptune data divided by five) at the bow shock increased by a factor of four, but at the termination shock by a factor of two. The major difference is in the temperature (**c**; Neptune data divided by two): at the bow shock it increased by a factor of 100, but at the termination shock by a factor of only ten. The differences between these two shocks are probably caused by the greater abundance of pickup ions at the termination shock.

Received 9 March; accepted 15 April 2008.

1. Decker, R. B. *et al.* Voyager 1 in the foreshock, termination shock, and heliosheath. *Science* **309**, 2020–2024 (2005).
2. Burlaga, L. F. *et al.* Crossing the termination shock into the heliosheath: magnetic fields. *Science* **309**, 2027–2029 (2005).
3. Stone, E. C. *et al.* Voyager 1 explores the termination shock region and the heliosheath beyond. *Science* **309**, 2017–2020 (2005).
4. Burlaga, L. F. *et al.* Magnetic fields at the solar wind termination shock. *Nature* doi:10.1038/nature07029 (this issue).
5. Decker, R. B. *et al.* Mediation of the solar wind termination shock by non-thermal ions. *Nature* doi:10.1038/nature07030 (this issue).
6. Gurnett, D. A. & Kurth, W. S. Intense plasma waves at and near the solar wind termination shock. *Nature* doi:10.1038/nature07023 (this issue).
7. Stone, E. C. *et al.* An asymmetric solar wind termination shock. *Nature* doi:10.1038/nature07022 (this issue).
8. Bridge, H. S. *et al.* The plasma experiment on the 1977 Voyager mission. *Space Sci. Rev.* **21**, 259–287 (1977).
9. Opher, M., Stone, E. C. & Liewer, P. C. The effects of a local interstellar magnetic field on Voyager 1 and 2 observations. *Astrophys. J.* **640**, L71–L74 (2006).
10. Pogorelov, N. V., Zank, G. P. & Ogino, T. Three-dimensional features of the outer heliosphere due to coupling between the interstellar and interplanetary magnetic fields. II. The presence of neutral hydrogen atoms. *Astrophys. J.* **644**, 1299–1316 (2006).
11. Lallement, R. *et al.* Deflection of the interstellar neutral hydrogen flow across the heliospheric interface. *Science* **307**, 1447–1449 (2005).
12. Izmodenov, V., Malama, Y. G. & Ruderman, M. Solar cycle influence on the interaction of the solar wind with Local Interstellar Cloud. *Astron. Astrophys.* **429**, 1069–1080 (2005).

13. Gurnett, D. A. & Kurth, W. S. Electron plasma oscillations upstream of the solar wind termination shock. *Science* **309,** 2025–2027 (2005).
14. Opher, M., Stone, E. C. & Gombosi, T. I. The orientation of the local interstellar magnetic field. *Science* **316,** 875–878 (2007).
15. Jokipii, J. R., Giacalone, J. & Kota, J. Transverse streaming anisotropies of charged particles accelerated at the solar wind termination shock. *Astrophys. J.* **611,** L141–L144 (2004).
16. Gloeckler, G., Fisk, L. A. & Lanzerotti, L. J. Acceleration of solar wind and pickup ions by shocks, in *Connecting Sun and Heliosphere (Proc. Solar Wind 11/SOHO 16 Conf.)* (eds Fleck, B., Zurbuchen, T. H. & Lacoste, H.) 107–112 (ESA, Noordwijk, 2005).
17. Zank, G., Pauls, H., Cairns, I. & Webb, G. Interstellar pickup ions and quasi-perpendicular shocks: Implications for the termination shock and interplanetary shocks. *J. Geophys. Res.* **101,** 457–477 (1996).
18. Lipatov, A. S. & Zank, G. P. Pickup ion acceleration at low-β_p perpendicular shocks. *Phys. Rev. Lett.* **82,** 3609–3612 (1999).
19. Giacalone, J. & Burgess, D. Hybrid simulations of the interaction of a current sheet with the termination shock. *Eos* 88 (Fall meeting), abstr. SH12B-05 (2007).
20. Pogorelov, N. V., Stone, E. C., Florinski, V. & Zank, G. P. Termination shock asymmetries as seen by the Voyager spacecraft: The role of the interstellar magnetic field and neutral hydrogen. *Astrophys. J.* **668,** 611–624 (2007).
21. Wang, C., Richardson, J. D. & Paularena, K. I. Predicted Voyager observations of the Bastille Day 2000 coronal mass ejection. *J. Geophys. Res.* **106,** 13007–13013 (2001).
22. Berdichevsky, D. B., Szabo, A., Lepping, R., Viñas, A. & Mariani, F. Interplanetary fast shocks and associated drivers observed through the 23rd solar minimum by Wind over its first 2.5 years. *J. Geophys. Res.* **105,** 27289–27314 (2000).
23. Vinas, A. F. & Scudder, J. D. Fast and optimal solution to the 'Rankine-Hugoniot problem'. *J. Geophys. Res.* **91,** 39–58 (1986).

Acknowledgements The work at MIT is supported by NASA. C.W. is grateful for support from NNSFC. Magnetic field data are shown courtesy of the Voyager magnetometer team (principle investigator N. Ness). We thank G. Gordon, Jr and L. Finck for development of and assistance with the plasma analysis.

Author Contributions J.D.R. analysed the plasma data and wrote the paper. J.C.K. performed the calculations for and write-up of the shock parameters. C.W. calculated the termination shock motion. J.W.B. and A.J.L. assisted with design of the instrument and manuscript preparation.

Author Information Data from the Voyager 2 plasma experiment are available at http://web.mit.edu/space/www/voyager.html. Reprints and permissions information is available at www.nature.com/reprints. Correspondence and requests for materials should be addressed to J.D.R. (jdr@space.mit.edu).